Hard X-Rays for In Situ Strain and Texture Measurements

Heinz-Günter Brokmeier*, **

(Received: 24 November 2008; in revised form: 25 March 2009; accepted: 26 March 2009; published online: 16 July 2009)

DOI: 10.1002/ppsc.200800050

Abstract

Hard X-rays having photon energies of higher than 50 keV are characterized by having a high penetration power. These high energy X-rays are provided by using W-tubes or at storage rings (synchrotron radiation). Due to the high photon flux and the excellent brilliance of synchrotron radiation, experiments can be carried out quickly. In situ strain experiments can be performed in real time, so that lattice strain evolutions can be investigated in parallel to obtaining conventional stress-strain curves. Crystallographic texture measurements are time consuming but quick synchrotron measurements at different points of the stress-strain curve are able to describe the texture evolution during tension or compression, allowing confirmation of texture simulations and yielding material property evolutions during tension or compression experiments.

Keywords: hard X-rays, high temperature, in situ loading, lattice strain, texture evolution

1 Introduction

Hard X-rays with energies higher than 50 keV are characterized by their high penetration length in most materials. A comparison of the penetration length for some common metals with four typical radiations, i.e., Cu-Kα–1.5418 Å, 100 keV synchrotron radiation – 0.124 Å, 200 keV synchrotron radiation – 0.062 Å, thermal neutrons 1.250 Å [1], is given in Table 1. The penetration power is given in cm for a loss of 50 % of the primary beam intensity. The advantages and disadvantages of hard X-rays, neutrons and soft X-rays (9keV Cu-Kα, 7 keV Co-Kα) ensure that these radiations are complementary for materials science investigations; for more detail see Brokmeier and Yi [2], Bunge [3], Spieß et al. [4], and Reimers [5]. Synchrotron radiation has been used intensively for diffraction experiments and tomography [6], in contrast to material testing tubes, which also have energies up to 450 keV and are mainly applied for radiography.

Table 1: Penetration power of different radiations for some metals.

Instrument	D 5000	BW5	Harwi-II	TEX-2
	Cu-Kα, 1.54 Å	s-ray, 0.124 Å 100 keV	s-ray, 0.062 Å 200 keV	n-ray, 1.00 Å
Mg	0.0014 cm	3.4 cm	4.2 cm	6.10 cm
Al	0.0053 cm	1.5 cm	2.7 cm	7.67 cm
Cu	0.0015 cm	0.2 cm	0.5 cm	0.85 cm
Ti	0.0011 cm	0.6 cm	1.3 cm	1.61 cm
Pb	0.0003 cm	0.03 cm	0.04 cm	2.10 cm

Texture development is among the major characteristics of materials processing which also includes deformation and recrystallization [7,8]. Standard texture investigations carried out to describe the successive states of a sample, imply that sets of samples with varying composition and thermo-mechanical parameters, e.g., deformation degree and temperature, annealing temperature and time, etc., always have to be measured. Dynamic investigations on magnitudes such as phase transformation, strain and texture development during annealing or applied loading require in situ methods. New experi-

* Prof. Dr. H.-G. Brokmeier, Institut für Werkstoffkunde und Werkstofftechnik, Technische Universität Clausthal, Agricolastrasse 6, 38678 Clausthal Zellerfeld (Germany).
E-mail: heinz-guenter.brokmeier@tu-clausthal.de

** GKSS-Forschungszentrum, Max-Planck-Str.1, Geb. 03, 21502 Geesthacht (Germany).

© 2009 WILEY-VCH Verlag GmbH & Co. KGaA, Weinheim

mental techniques and new instruments at large-scale facilities (both neutron and synchrotron) allow for much faster measurements. They are absolutely necessary for in situ experimentation due to the presence of creep or recrystallization processes.

A brief description is given for in situ texture experiments carried out at the high energy beamline BW5 at Hasylab/DESY (Hamburg) by using case study examples. In contrast to in situ strain measurements, which are much more common, texture measurements are time consuming, so that the number of this type of experiments performed is still low. In order to describe the influence of the initial texture on the anisotropy of materials, in situ texture analyses can be interpreted by texture simulations, e.g., VPSC model or crystal plasticity model, but this is not part of the present study. Loading experiments comparable to standard material tests, i.e., stress-strain curves, were carried out on aluminium and magnesium-alloys in tension mode as well as in compression mode using a 20 kN loading device. Due to the high penetration length of 100 keV X-rays, DIN 50125 samples of 6 mm in diameter were used in transmission mode. In addition to standard texture measurements at the initial state and after failure, up to five points of the known stress-strain curve were chosen for in situ texture measurements. An image plate detector covers a set of complete Debye-Scherrer cones, so that only ω-scans are necessary to obtain complete pole figures and the entire experiment is very quick. It is even fast enough to perform high temperature experiments, which are very sensitive, time-dependent reactions. Two types of furnace are available, one which can be combined with the loading device and the other which is a stand alone furnace. A phase and texture transition takes place during processing in many materials. Another example from the current authors describes the first in situ high temperature experiment on a steel sample to investigate the phase and texture transition (ferrite-austenite).

2 Experimental Equipment

The work horse instrument for the in situ experiments, presented in this paper, was the high energy beamline BW5 at Hasylab/DESY (Hamburg) [8]. The typical layout of such a diffractometer is shown in Figure 1. The basic components are a monochromator, a sample stage for standard sample geometries as well as for additional equipment such as furnaces, loading devices and area detectors.

A new materials science beamline (Harwi II) operated by the GKSS-Research Center complements the instrumentation using high energy X-rays at the Doris III storage ring at Hasylab/Desy Hamburg. When using a two-dimensional image plate detector (MAR345), one to five seconds is the typical exposure time required to obtain a high quality image plate picture, as shown for a corundum powder in Figure 2. Due to the high photon energy and the low wavelength, relatively small scattering angles are possible. Consequently, a set of 15 complete Debye-Scherrer rings are detected simultaneously in a 2θ range of ca. 8°. It should be noted that a glass cylinder of 8 mm in diameter was filled with corundum powder without any preferred orientation. One can see clearly that the Debye-Scherrer cones in the powder sample show homogeneous intensity distributions along the different rings. This indicates good grain statistics and, simultaneously, a random distribution of the grains.

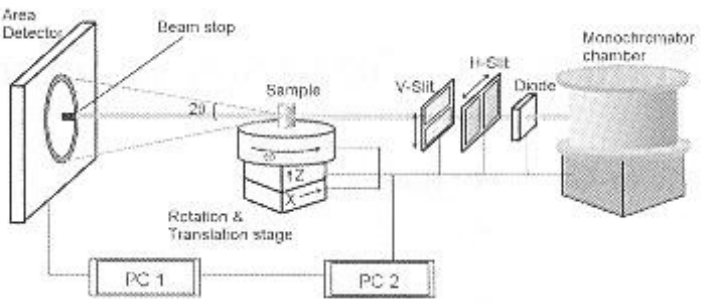

Fig. 1: Layout of the high energy beamline BW5 at Hasylab / Desy (Hamburg).

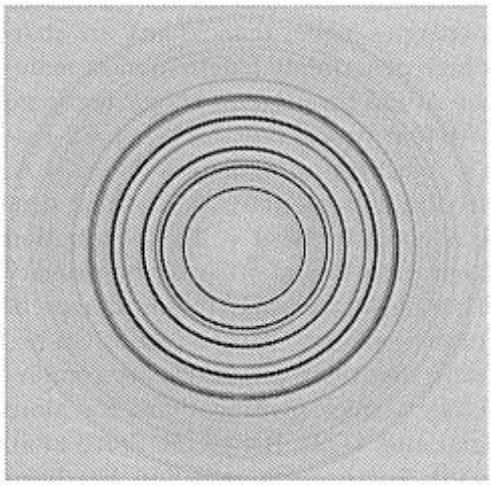

Fig. 2: Image plate pictures of corundum powder.

Due to thermo-mechanical processing, most samples have a preferred orientation that is visible for a titanium-aluminide sample in the intensity distribution along the different Debeye Scherrer rings (see Figure 3a). This sample of cubic shape (14 mm thickness) was fine grained (see Figure 3b) with excellent grain statistics because of the dense arrangement of the intensities along the Debye-Scherrer rings.

© 2009 WILEY-VCH Verlag GmbH & Co. KGaA, Weinheim

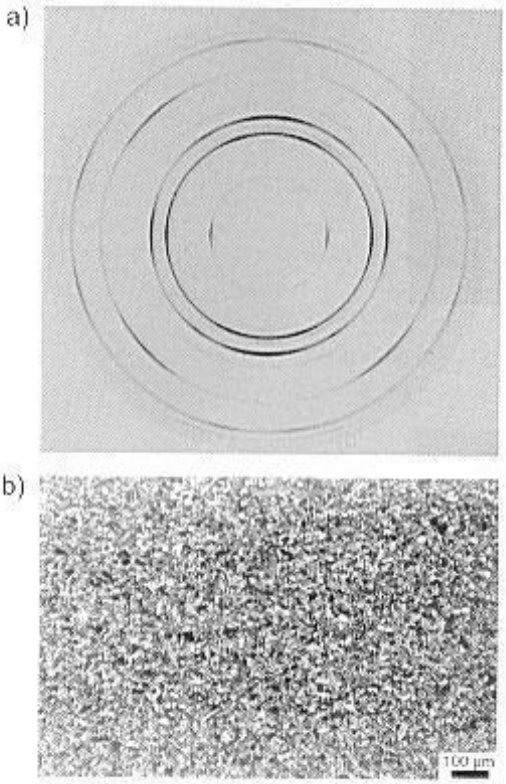

Fig. 3: Image plate pictures a), and microstructure b), of fine grained titanium aluminide.

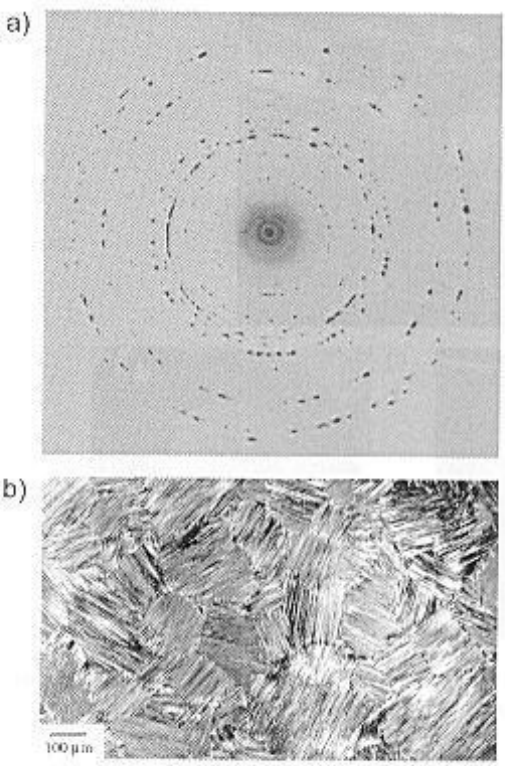

Fig. 4: Image plate pictures a), and microstructure b), of coarse grained titanium-aluminide.

In cases of coarse grained materials, the grain size statistics can be insufficient and spotty intensity distributions can result. Figure 4 shows such an example of a coarse grained titanium-aluminide sample, with both, the image plate (Figure 4a) and the microstructure (Figure 4b) shown.

The in situ measurement of crystallographic texture is a different type of a non-destructive measurement, which requires special equipment. Due to the high photon flux and the excellent brilliance, high energetic sources of synchrotron radiation are a fantastic tool, particularly for fast experiments. Moreover, the high penetration power of these hard X-rays (50 to 200 keV) allows the investigation of standard tensile samples defined by the DIN-norm. A loading device with a power up to 20 kN was used at the hard wiggler beamline BW5 (HASYLAB-DESY) to perform in situ strain and in situ texture analysis. One obtains short wavelengths using 100 keV X-rays, so that a 2D image-plate detector offers a wide range of diffraction patterns within the first 10° in 2θ. Rectangular extruded Mg-AZ31 was investigated by an in situ tensile experiment. Samples were cut at 0°, 45° and 90° to the extrusion direction [9]. In situ strain studies show that the lattice dependent strains are perpendicular and parallel to the loading direction. Moreover, in hexagonal Mg-AZ31, a strong influence of the initial texture on the tensile behavior can be explained by a combination of texture simulation with in situ measurements. An initial experiment with steel at high temperature was performed to measure the texture evolution occurring together with the phase transition. Three different types of in situ devices are shown in Figure 5 (see also Brokmeier et al. [10]).

3 Experiments and Examples

3.1 Texture Measurement by Synchrotron Radiation

The basic method for pole figure measurement using synchrotron radiation follows film techniques that have been standard since the beginning of the 1960s [11, 12, 13]. Film techniques use an area detector (film) with gray scale analysis to obtain the intensities. New area detectors such as image plates or CCD cameras provide direct pixel dependent information of the scattered intensities. Due to the high brilliance of the synchrotron source, texture measurement using synchrotron radiation is very efficient for fast measurements, for local investigation [14, 15] and for in situ studies [16]. The basic principles of pole figure measurement using synchrotron radiation with an area detector are described in detail by Brokmeier and Yi [2], (see Figure 6). In order to obtain a complete pole figure one has to col-

© 2009 WILEY-VCH Verlag GmbH & Co. KGaA, Weinheim

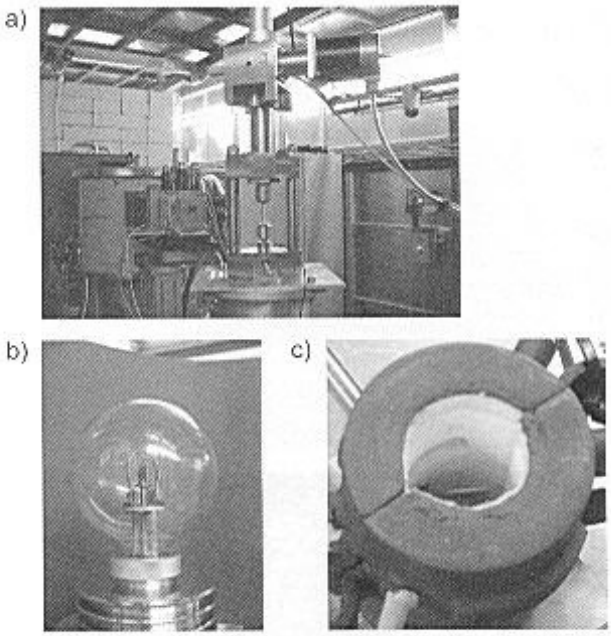

Fig. 5: Equipment for in situ experiments: a) 20 kN loading device, b) dome furnace, and c) cylindrical furnace for the loading device.

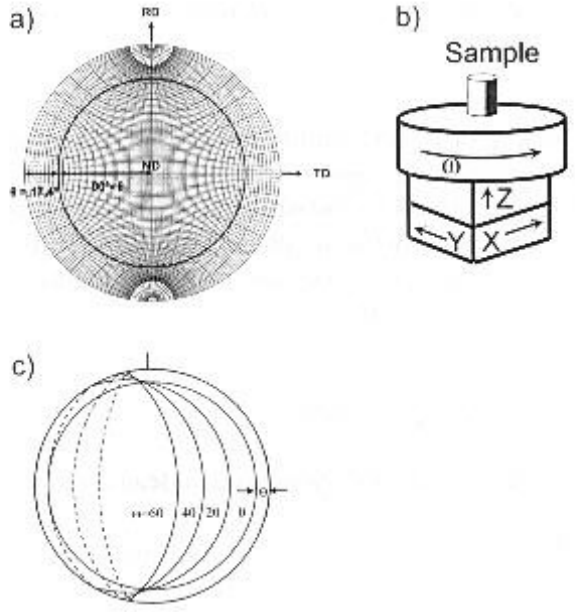

Fig. 6: a) pole figure with the projection of one Debye-Scherrer ring with $\theta = 17.4°$, b) sample table with only one ω-rotation table, and c) projection of the Debye-Scherrer ring for different ω-rotations.

lect a set of image plate pictures for different ω-rotations.

Two examples of a single shot at $\omega = 0°$ and a complete pole figure measured from $\omega = -90°$ to $+90°$ with $\Delta\omega = 5°$ are shown in Figure 7. The first example is a magnesium (Mg) sample following a tensile test. One can see the broken portion inside a sample holder, Figure 7a). The texture at the fracture region can be measured with a

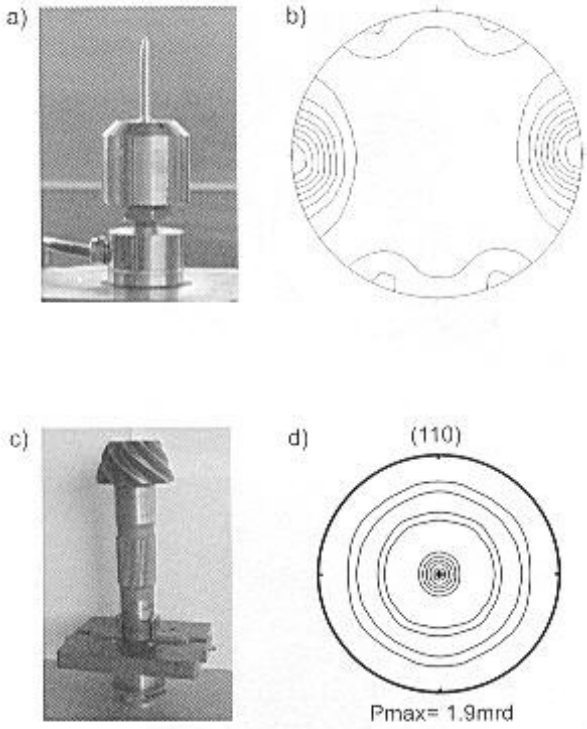

Fig. 7: Examples of pole figure measurement with hard X-rays. a) Mg sample after tensile test, b) (0006) pole figure, c) steel shaft, and d) (110) pole figure of iron.

synchrotron beam cross section of 1 mm^2. The basal plane pole figure (0006) is shown in Figure 7b). Sample 2 demonstrates the high penetration power of hard X-rays. A steel shaft of varying diameter between 22 mm and 35 mm (see Figure 7c) can be analyzed despite the strong absorption. This is possible due to the high photon flux, as shown for the Fe (110) pole figure in Figure 7d). It should also be noted that the counting time varies from 5 s for the Mg sample to 30 s for the steel sample.

One option that has been developed by Bunge et al. to follow texture changes [14], is the so-called 'moving detector method', which is based on a direct correlation of the detector movement with a sample state parameter such as temperature. The disadvantage of the technique is that only a part of one Debye-Scherrer cone can be used, which is obtained by a slit system. The combination of detector movement with an automatically controlled temperature increase provides the texture evolution during recrystallization for one pole figure. Different modes of this method allow the measurement of texture gradients or of dynamic recrystallization processes. Further details of this technique are provided by Bunge et al. [14]. Another option is to combine the conventional pole figure measurement with a loading device [18]. The conventional method is based on the collection of a sufficient number of pole figure intensities in a step size mode. The number of steps depends

© 2009 WILEY-VCH Verlag GmbH & Co. KGaA, Weinheim

on the pole figure window and the texture sharpness. Sharp textures require finer counting grids than weak textures.

3.2 In Situ Lattice Strain Measurement

The goal of the present activities is to improve the available in situ experimental methods to match material processing speeds, e.g., heating, tension, compression, and torsion. This is a new application of an in situ loading device using synchrotron radiation. In the first step, the diffraction pattern of Mg-powder was used to determine the X-ray wavelength to 0.1366 Å, which is always necessary to calibrate the instrument with a random sample before running the actual in situ experiment. A tensile sample cut from an extruded bar of Mg-AZ31 was tensioned at room temperature with a loading ram speed of 0.0018 mm/s. The Debye-Scherrer cones were registered at the beginning and under continuously increasing loading conditions. Figure 8a) shows the stress-strain curve. The dots express the points at different macro strain levels where the diffraction pattern were taken. The sample strain and the load were obtained in parallel so that a correlation of the macroscopic strain and the lattice strain is possible. Therefore, fundamental investigations of material properties can be carried out to characterize new alloys. Figures 8b) shows the sample orientation of the tensile sample with $\sigma_{parallel}$ and $\sigma_{perpendicular}$.

A detector image from the unstrained initial sample and the geometrical relationship between the sample direction and the detector image are shown in Figure 8c). The diffraction profile from the horizontal (vertical) line on the detector image represents the crystallographic planes perpendicular (parallel) to the loading axis. Figure 9 also presents the evolution of internal strains for different {hk.l} during tensile loading. Due to the texture of the present sample, it was possible to evaluate three diffraction peaks in the loading direction, i.e., {10.0}, {10.1} and {11.0}. Since the internal strains parallel to the loading axis are more constrained by external boundary conditions, the internal strains in this direction show greater agreement with the stress-strain curve. The internal strains on {10.1} parallel to the loading axis show earlier micro-yielding at 0.7 % of sample strain. On the other hand, the internal strains on {10.0} and {11.0} parallel to the loading axis show later micro-yielding at about 1.5 % of sample strain. The ratio of the internal strain on {10.0} and {10.1} is 2.4. This means that the dislocation gliding on the {10.1} plane, the so called soft-orientation, occurs more easily on this plane than on other

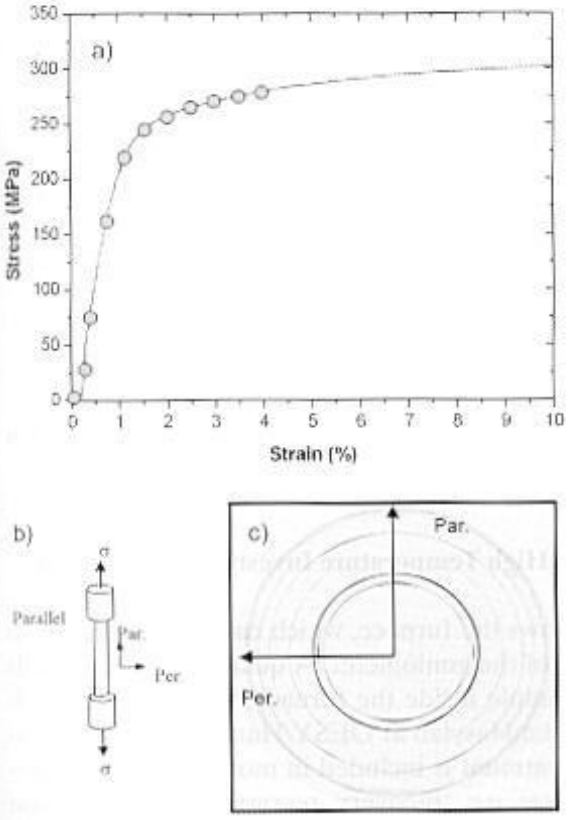

Fig. 8: a) stress-strain curve with measurement positions for lattice strain measurements, b) tensile sample with orientation marks, and c) image plate picture of Mg-AZ31 (unstrained).

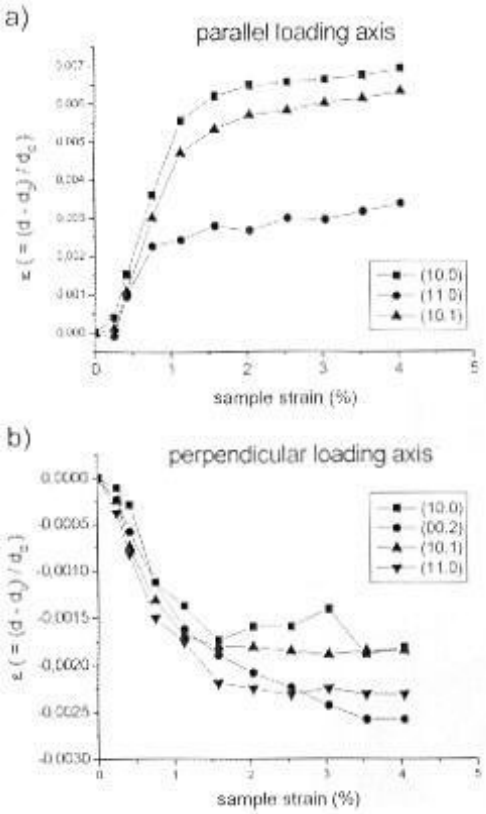

Fig. 9: Lattice dependent strain a) parallel, and b) perpendicular to the loading axis.

© 2009 WILEY-VCH Verlag GmbH & Co. KGaA, Weinheim

planes. In addition, the crystallographic planes perpendicular to the loading axis, which are under compression, clearly show the anisotropic response of internal strains, although the ratio of maximum and minimum internal strains is smaller than in the case for strain parallel to the loading axis. The {00.2} plane perpendicular to the loading axis shows the hardest behavior, while {10.1} has the softest response for the internal strains.

3.3 In Situ Texture Measurements on an Aluminium Sample

Texture measurement is a much slower technique than lattice strain measurement. Therefore, this measurement cannot be undertaken continuously. The loading experiment has to be stopped, while the texture measurement is performed under constant load. The loading curve is shown together with the 4 holding positions for texture measurements in Figure 10a). Firstly, the texture was measured in the unloaded state, and secondly, loading to 1.5 % strain was undertaken with subsequent texture analysis. The third and fourth steps were performed at 9.7 % strain (position 3) and at 20.3 % strain (position 4), respectively. The rectangular tensile sample can be seen in Figure 10b). Typically, a texture measurement takes between 60–90 min for one position.

Data analysis was performed in a conventional manner using the iterative series expansion method. However, due to the walls of the loading device, only incomplete pole figures can be measured. The walls provide a restriction in ω-rotation between –70° and +70°. However, due to the iteration procedure in the series expansion calculation, incomplete pole figures can be conveniently processed. Further details about the iterative serious expansion calculation are given elsewhere by Dahms and Bunge [18]. The texture itself and the texture evolution during loading will be presented in more detail in another paper. As shown by Yi [9], in situ texture evolution during loading is an excellent tool for making comparisons with texture simulations. Furthermore, anisotropic physical properties such as the elastic modulus or Young's modulus can be calculated from the quantitative texture data [19]. As an example, the evolution of planar and normal anisotropy during loading up to 20.3 % strain is shown in Figure 11. Due to the load induced texture change, a minor modification of rm-normal anisotropy and Δr-planar anisotropy can be seen.

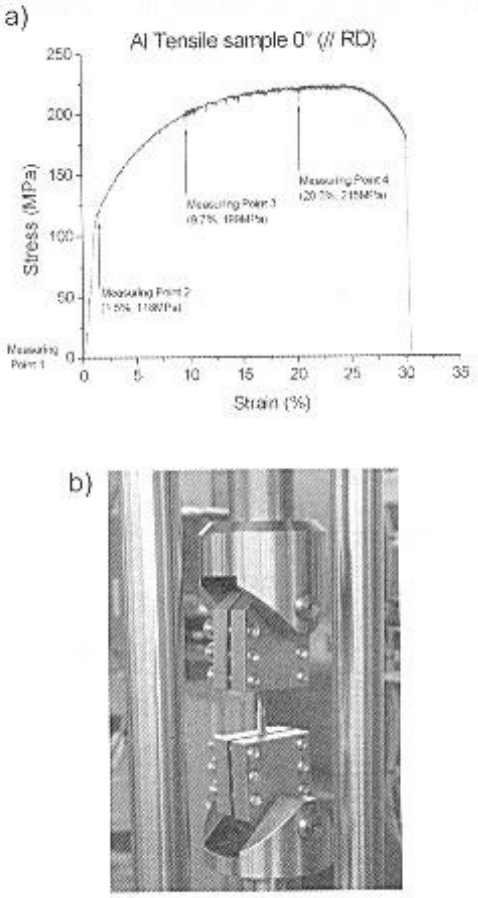

Fig. 10: Stress-strain curve for in situ texture analysis a), and tensile sample mounted in the loading device b).

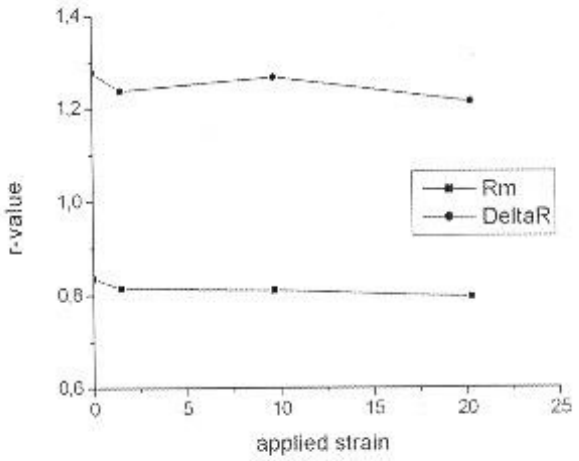

Fig. 11: Evolution of normal (rm) and planar (Δr) anisotropy of an Al sheet during in situ loading.

3.4 In Situ High Temperature Investigations on Steel

Figure 5 shows the furnace, which can be positioned on the ω-stage of the goniometer. A quartz dome surrounds the small sample inside the furnace, which was a development of the Hasylab at DESY/Hamburg. A high temperature treatment is included in more or less all industrial processes, e.g., recovery, recrystallization or phase transition. Thus, high temperature phase analysis by X-rays or neutrons is very common. However, high temperature texture analysis is restricted due to a much

© 2009 WILEY-VCH Verlag GmbH & Co. KGaA, Weinheim

longer total counting time. New instrumentation on high flux beams offers the possibility of measuring complete textures in less than 60 min. Recent developments have reduced the measuring time for a complete texture analysis to 10–20 min. Test experiments were carried out to study phase transformation in Ti-alloys, steel and shape memory alloys, to investigate the thermal expansion coefficient in Mg-alloys and in steel and to make a high temperature texture measurement on steel. The investigated test sample was composed of ST37K steel with a chemical composition of 0.10 C, 0.01 Si, 0.72 Mn, 0.027 P, and 0.027 S balanced Fe. A 5×5 mm^2 sample of steel of height 10 mm was prepared for the synchrotron measurement. In order to minimize the total counting time, a set of 9 image plate pictures with different ω angles were taken at each temperature. The exposure time was 1 s and the readout time was ca. 60 s. The reduced number of image plate pictures is possible because of the orthorhombic texture symmetry. The diffraction pattern for one ω-position and three temperatures are shown in Figure 12.

The program package MAUD (Materials Analysis Using Diffraction) [20] offers on the one hand, the determination of crystallographic and microstructure data (volume fraction, grain size and strain) using a Rietveld refinement and on the other hand, a quantitative texture analysis using a WIMV texture program. Thus, it was possible to determine the thermal expansion coefficients of α-ferrite, the phase transition (α-ferrite to γ-austenite), the volume fractions in the two-phase region and the texture transition [21]. Moreover, the texture transition of α-ferrite at room temperature to the high temperature γ-austenite phase is shown in Figure 13 for ferrite and in Figure 14 for austenite.

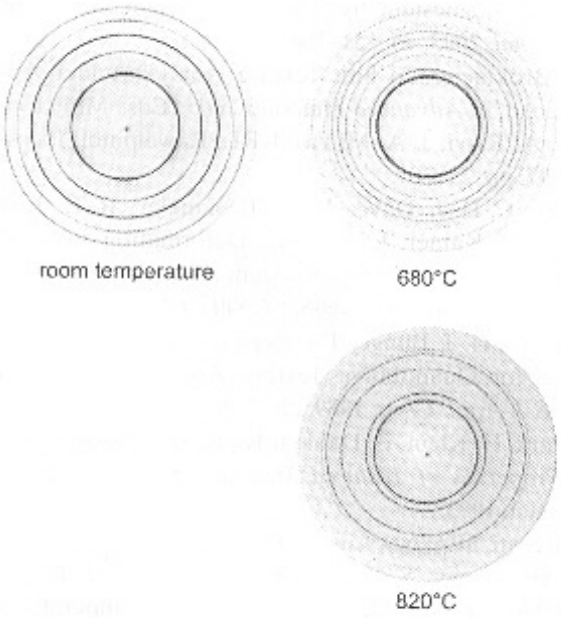

Fig. 12: Diffraction pattern of ST37K at room temperature, at 680 °C and at 820 °C.

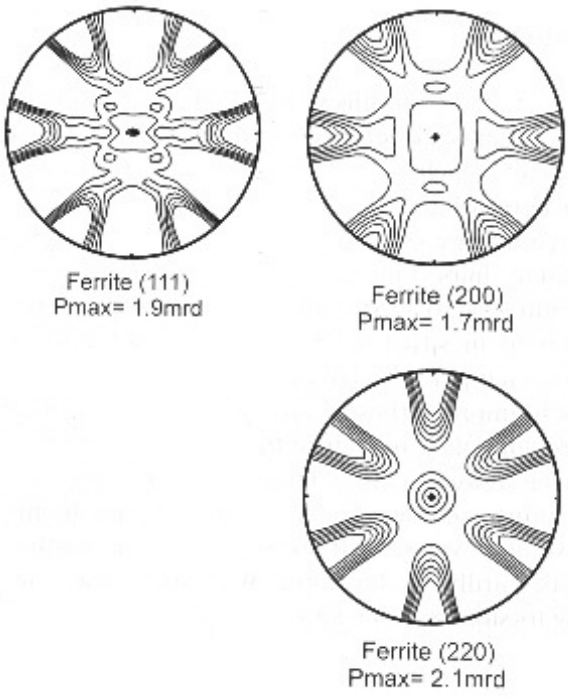

Fig. 13: Ferrite pole figures measured at room temperature (counter levels 1.0, 1.1, 1.2, 1.3 ...).

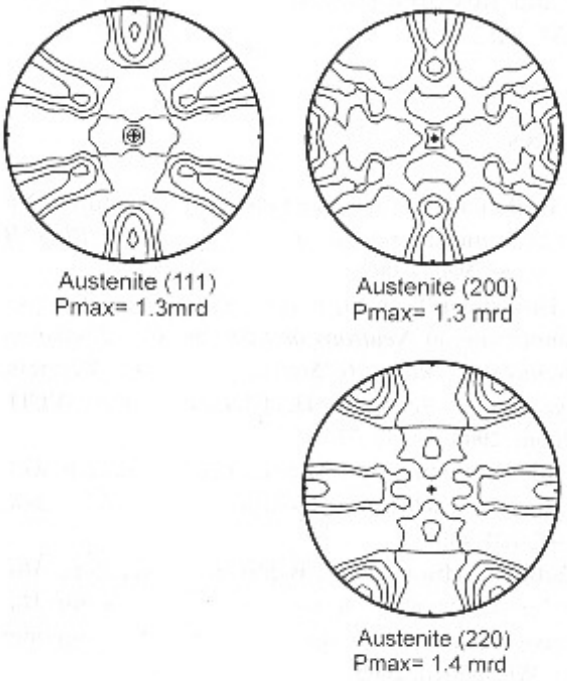

Fig. 14: Austenite pole figures measured at 820 °C (counter levels 1.0, 1.1, 1.2, 1.3 ...).

© 2009 WILEY-VCH Verlag GmbH & Co. KGaA, Weinheim

From a comparison of the high temperature austenite texture measured at 820 °C with the room temperature ferrite texture, one can conclude that in the current case, the $\alpha \Leftrightarrow \gamma$ transformation follows the Kurdjumov-Sachs model, i.e., $(111)\gamma // (011)\alpha$.

4 Conclusions

It can be concluded from this work that high technology texture instruments, developed at large-scale facilities, independent of which technique (energy dispersive or angular dispersive) or which radiation (thermal neutrons or high energy synchrotrons) is used, are playing an increasingly important role in crystallographic texture determination. The present work provides a brief introduction to in situ texture analysis under applied load and high temperature conditions. Investigations are in progress to improve these techniques. The first aim of these improvements is to reduce the total counting time by employing more effective detector systems and time saving scanning routines. Secondly, it is hoped to improve existing devices such as furnaces and loading devices and, thirdly, to develop new in situ devices for monitoring torsion, welding and melting.

5 Acknowledgements

This work has been funded by the German Ministry of Education and Research (BMBF) under contract number 05KS1MCA/2.

6 References

[1] H.-G. Brokmeier, Global Crystallographic Textures Obtained by Neutron and Synchrotron Radiation, *Phys. B (Amsterdam, Neth.)* **2006**, *385–386*, 623–625.

[2] H.-G. Brokmeier, S.-B. Yi, Texture and Texture Analysis in Engineering, in *Neutrons and Synchrotron Radiation in Engineering Materials Science* (Eds.: W. Reimers, A. Pyzalla, A. Schreyer, H. Clemens), Wiley-VCH, Weinheim, **2008**, pp. 57–77.

[3] H. J. Bunge, Texture and Microstructure Analysis with High-Energy Synchrotron Radiation. *Adv. X-Ray Anal.* **2004**, *47*, 420–430.

[4] L. Spieß, R. Schwarzer, H. Behnken, G. Teichert, *Moderne Röntgenbeugung: Röntgendiffraktometrie für Materialwissenschaftler, Physiker und Chemiker*. Teubner Verlag, Wiesbaden, **2005**.

[5] W. Reimers, Introduction to Diffraction Methods for Internal Stress Analyses, in *Neutrons and Synchrotron Radiation in Engineering Materials Science* (Eds.: W. Reimers, A. Pyzalla, A. Schreyer, H. Clemens), Wiley-VCH, Weinheim, **2008**, pp. 115–136.

[6] F. Beckmann, Neutron and Synchrotron-Radiation-based Imaging for Applications in Materials Science – from Macro- to Nanotomography, in *Neutrons and Synchrotron Radiation in Engineering Materials Science* (Eds.: W. Reimers, A. Pyzalla, A. Schreyer, H. Clemens), Wiley-VCH, Weinheim, **2008**, pp. 287–308.

[7] H.-F. Kocks, C. Tome, H. R. Wenk, *Texture and Anisotropy*. Cambridge University Press, Cambridge, **1998**.

[8] L. Weislak, J. R. Schneider, Th. Tschentscher, H. Klein, H. J. Bunge, Hard X-Ray Texture Measurements with an Online Image Plate Detector, *Nucl. Instr. Methods Phys. Res. Sect. A* **2001**, *467–468*, 1257–1260.

[9] S. B. Yi, *Investigation on the Deformation Behavior and the Texture Evolution in Magnesium Wrought Alloy AZ31*, PhD Thesis, Technische Universität Clausthal, **2005**.

[10] H.-G. Brokmeier, S.-B. Yi, J. Homeyer, In Situ Analysis of Crystallographic Textures using High-Energy X-Rays, *Arch. Metall. Metals* **2008**, *53*, 33–38.

[11] J. F. H. Clusters, Betrachtung über Metalltexturen, *Philips Tech. Rundschau* **1942**, *7*, 13–20.

[12] G. Wassermann, J. Grewen, *Texturen Metallischer Werkstoffe*. Springer Verlag, Berlin, **1962**.

[13] H. R. Wenk, Eine photographische Röntgengefügeanalyse, *Schweiz. Min. Petr. Mitt.* **1965**, *45*, 518–550.

[14] H. J. Bunge, H. Klein, L. Weislak, U. Garbe, W. Weiss, J. R. Schneider, High-Resolution Imaging of Texture and Microstructure by the Moving Detector Method, *Texture Microstruct.* **2003**, *35*, 253–271.

[15] H.-G. Brokmeier, A. Günther, S. Yi, W. Ye, T. Lippmann, U. Garbe, Investigation of Local Textures in Extruded Magnesium by Synchrotron Radiation, *Adv. X-Ray Anal.* **2003**, *46*, 151–156.

[16] H.-G. Brokmeier, In Situ Texture Analysis under Applied Load, in *Advanced Materials 2005* (Eds.: M. Farooque, S. A. Rizvi, J. A. Mirza), KRL, Rawalpindi, Pakistan, **2007**, pp. 29–301.

[17] S.-B. Yi, C. H. J. Davis, H.-G. Brokmeier, R. E. Bolmaro, K. U. Kainer, J. Homeyer, Deformation and Texture Evolution in AZ31 Magnesium Alloy during Uniaxial Loading, *Acta Mater.* **2006**, *54*, 549–562.

[18] M. Dahms, H. J. Bunge, The Iterative Series Expansion Method for Quantitative Texture Analysis. I. General Outline, *J. Appl. Cryst.* **1989**, *22*, 439–447.

[19] N. J. Park, H. Klein, E. Dahlem-Klein, H. J. Bunge, *Physical Properties of Textured Materials*. Cuvillier Verlag, Göttingen, **1993**.

[20] L. Lutteroti, http://www.ing.unitn.it/~maud/.

[21] H.-G. Brokmeier, S.-B. Yi, J. Homeyer, Texture Transition in Steel, In Situ Measurement at High Temperatures using High-Energy X-Rays, in *Texture and Microstructure of Steels* (Eds.: A. Haldar, S. Suwas, D. Bhattacharjee), Springer Verlag, Berlin, **2008**.

© 2009 WILEY-VCH Verlag GmbH & Co. KGaA, Weinheim